A protecting group approach toward synthesis of Au-silica Janus nanostars

This item is the archived peer-reviewed author-version of:

Title: A protecting group approach toward synthesis of Au-silica Janus nanostars

Authors: Rodríguez-Fernández Denis, Altantzis Thomas, Heidari Mezerji Hamed, Bals Sara, Liz-Marzan Luis M.

In: ChemComm (2014)

To refer to or to cite this work, please use the citation to the published version:

A Protecting Group Approach toward Au-Silica Janus Nanostars

Denis Rodríguez-Fernández[a,c] **, , Thomas Altantzis**[b] **, Hamed Heidari** [b] **, Sara Bals**[b]**, Luis M. Liz-Marzán**[a,c,d]

Patchy and Janus particles offer new opportunities toward multifunctionality and directed assembly. Although colloid chemistry methods have been reported, these were mainly applied to sub-micron particles and not easily implemented for
10 **nanoparticles. We demonstrate here the synthesis of Janus nanoparticles comprising a silica hemisphere and a gold semistar. The synthetic method relies on the application to colloid chemistry the concept of protection groups widely employed in organic chemistry, so that gold branches can only grow on half of**
15 **a seed sphere. The asymmetric metallic-inorganic structure of these nanoparticles was characterized by electron tomography and aberration corrected transmission electron microscopy. This configuration opens new possibilities to apply the plasmonic properties of gold nanostars e.g. for SERS detection, together**
20 **with the wide variety of chemical functionalization of the silica component.**

Protecting groups are commonly used in organic chemistry to perform chemical reactions in the presence of other functional groups that can be affected by the process. The quest of new
25 protecting groups with multiple properties has led synthetic protocols to a new level that allows the preparation of highly complex molecules.[1] Although protection and deprotection have been widely employed with great success at the molecular level and even with colloids larger than 100 nm, this strategy has been
30 far less explored with small nanoparticles.[2,3,4,5] Various molecular analogies have been proposed for the design of novel nanoscale materials, and in particular for plasmonic nanomaterials.[6] However, whereas in organic chemistry these processes are mainly carried out in homogeneous solutions and the final
35 products are obtained by routine techniques such as crystallization or chromatography and solvent evaporation, when working with colloids different parameters must be considered e.g. to avoid aggregation during synthesis and recovery of the product, including the type of solvent, the nature of the
40 nanoparticles or the stabilizing molecules, among others.

We present here a protecting group-like strategy to synthesize Janus nanoparticles, exhibiting different materials on roughly each half of the particle. Our objective was to achieve plasmonic nanoparticles that could be functionalized differently at opposite
45 sides, while maintaining a strong optical (plasmonic) activity, for example gold nanostars[7] in which the spikes protrude from only one half of the central sphere. Such a configuration may offer important advantages toward subsequent directed self-assembly processes or selective biofunctionalization. We thus devised a
50 multistep procedure involving several pathways that have been previously used to synthesize patchy particles: self-assembly of ligands over a metallic surface, masking or protection and seeded

growth.[8] We first prepared 40 nm gold nanoparticles, onto which two different ligands were self-assembled to guide the growth of
55 a silica semishell, leading to the formation of Au-SiO₂ Janus particles. Besides providing colloidal stability due to a high negative charge, the silica semishell acted as a mask to direct the subsequent seeded growth of gold spikes exclusively on the part of the metal that remained exposed to the solution. This
60 ultimately leads to a particle comprising a silica quasi-sphere with Au branches protruding from one side and therefore with highly anisotropic optical properties. Finally, the silica shell can be also removed if required, thus completely mimicking the behavior of protecting groups in organic chemistry. This
65 approach is summarized in *Figure 1* and full details are provided in the *Electronic Supporting Information* (*ESI*).

Also shown in *Figure 1* are representative TEM images corresponding to the different synthesis steps (Vis-NIR spectra are shown in *Figures S2 and S3*, *ESI*). First ca. 40 nm citrate-
70 capped Au spheres (λ_{max}~528nm) were prepared,[9] which could be easily transferred into organic solvents for the growth of the silica semishells, probably due to the high concentration of citrate molecules compared to previous methods.[10] Prior to formation of
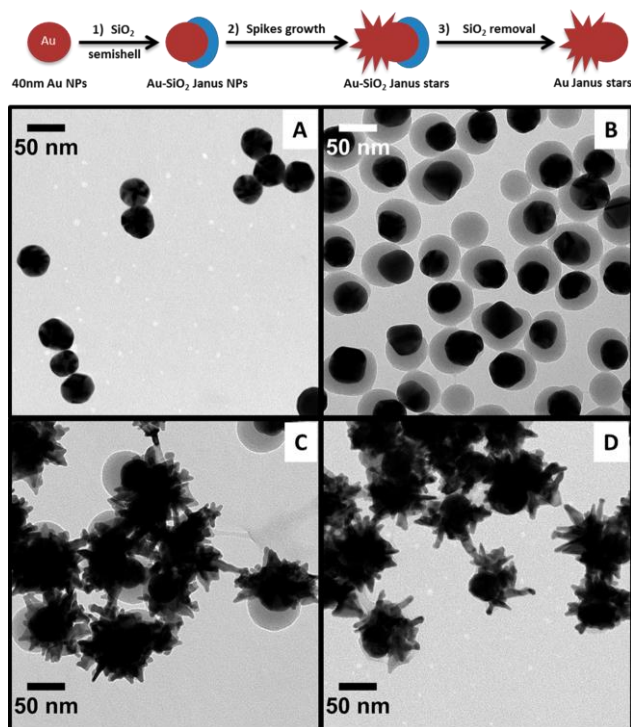

Fig. 1. Representative TEM micrographs **of**: ~40nm Au@citrate (A); Janus Au-SiO₂ (B)**;** Au-SiO₂ Janus nanostars **(C);** and Au Janus nanostars after SiO₂ removal (D). See low magnification images in *Figure S1* (ESI).

the oxide layer, in a 2-propanol:water mixture (2:1) a ligand couple – 4-mercaptobenzoic acid (4-MBA) and poly-(acrylic acid) (PAA, Mw=25000g/mol) – were self-assembled over the metallic surface, resulting in significant segregation.[11] Silica was then formed by means of the well-known Stöber method on top of the 4-MBA-capped area, while PAA acted as a stabilizer over the exposed gold surface (*step 1, Figure 1*). These particles were stable in the synthesis solution, but could also be washed with 2-propanol to remove the excess of reactants with no apparent aggregation or particle degradation. Typical TEM images and Vis-NIR spectrum (λ_{max}~535nm) are shown in *Figure 1B* and *S2*, respectively. The TEM micrographs nicely show the formation of silica semishells on the Au cores, with minor silica nucleation, which did not affect the subsequent synthesis steps, while the plasmon band shows a small redshift due to changes in the local refractive index around the Au nanoparticle core.[12] The SiO_2 semishell was subsequently used as a hard mask to protect part of the surface toward the further growth of Au spikes (*step 2, Figure 1*). After centrifugation and washing with pure water to remove excess reactants, Au spikes were grown using a surfactant free approach, where L-ascorbic acid acts as a weak reducing agent in the presence of silver and hydrochloric acid.[13] Since this method avoids the use of surfactants and polymers, exchange of the remaining PAA is not needed and the obtained branched structures display a rather clean surface, which makes them ideal candidates for self-assembly or surface enhanced Raman scattering (SERS), where subsequent functionalization is usually required.[14,15,16,17,18,] Au-SiO_2 Janus nanostars were obtained in less than one minute and collected by centrifugation. It has been reported that, after a certain period of time a reshaping process takes place on nanostars leading to less spiky structures, indicated by a plasmon band blueshift.[19] In these surfactant-free stars this process was observed within a couple of days and additionally silica was found to dissolve if the particles are stored in aqueous medium after the synthesis (see *Figures S3* and *S4*).[20] However, both processes can be prevented by transferring the particles to an ethanol solution containing 4-MBA 20 μM and washing several times with pure ethanol to remove unattached 4-MBA molecules. As can be observed in *Figure 1C*, the silica shell and the spikes are clearly present in particles prepared in this way. The choice of 4-MBA relies on the well-known adsorption of thiol molecules over metal surfaces, which prevents other surface phenomena from occurring, as reflected in the stability of the gold spikes, which remained unchanged for at least three months. Storage of Au-SiO_2 Janus stars in water without addition of 4-MBA however leads to less spiky structures and silica dissolution within a few days (see *Figure S4*). Oppositely, upon addition of 4-MBA in water Au Janus nanostars are obtained, i.e. the Au branches are preserved while the silica protecting mask is removed (*step 3, Figure 1*). A representative TEM image of the Au Janus nanoparticles is shown in *Figure 1D*, where the gold branched part can be seen next to a smooth hemisphere.

Since conventional TEM images only provide 2D projections of 3D objects, more detailed characterization was carried out by high-angle annular dark field scanning transmission electron microscopy (HAADF-STEM) tomography (*see rendered movies in ESI*) and aberration corrected, high resolution HAADF-STEM to clarify their morphology. Two examples are shown in *Figure 2*
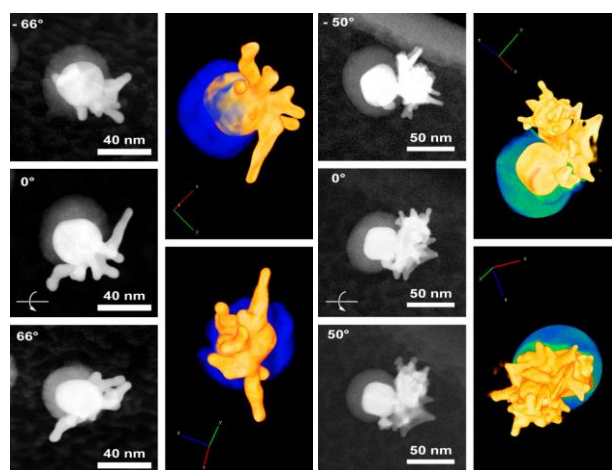

Fig. 2. HAADF-STEM images used for tomographic reconstruction acquired at different angles and the corresponding rendered 3D reconstructions along different viewing directions showing the Au parts in yellow and the SiO_2 shells in blue, for two different Au-SiO_2 Janus stars (left: short branches; right: large branches).

for Au-SiO_2 Janus nanostars with short and long branches, for which we display HAADF-STEM images obtained at different angles, together with the corresponding rendered 3D images. Silica is represented in blue and the metallic part in golden colour. These images clearly confirm that the gold spikes only grow from the exposed face of the metal, which is not covered by the silica hard mask (protecting group). Whereas for short spikes random orientation from the central core is observed, in the long branched nanoparticles, obtained when using lower amount of seeds, the 3D structure suggests that secondary branching occurred on few spikes that were initially grown. This cannot be observed in the common TEM projection images, so HAADF-STEM tomography is an essential tool to understand this type of systems. Tomography was also used to image the Janus nanostars after dissolution of the silica layer, again clearly showing a highly branched side which is well differentiated from a quasi-spherical side in the particle (*see Figure S5*).

A final piece of information regarding the ultrastructure of these unusual nanoparticles was provided by high resolution HAADF-STEM, as exemplified in *Figure 3*. A HAADF-STEM picture of a single Au-SiO_2 Janus star with small branches is shown in *Figure 3A*, revealing the presence of a spherical gold particle with spikes (brighter areas) and a silica semishell (less bright area). The more detailed image of the same particle in *Figure 3B* indicates that the gold core is multiply twinned, as expected for such large quasi-spherical particles, whereas the images in *Figure 3C-D* show the branching part from the core for several spikes, indicating that they are single crystalline, at least in a first stage. Paying more attention to the edge of the spike in *Figure 3D*, a deviation from the zone axis orientation can be seen, so highly branched particles might exhibit different crystallographic orientations where secondary spikes grow over previous branches. A similar analysis was carried out on particles with larger branches (*see Figure S6*), but in this case the overlap between different parts of the particles makes it difficult to distinguish the corresponding crystallographic orientations.
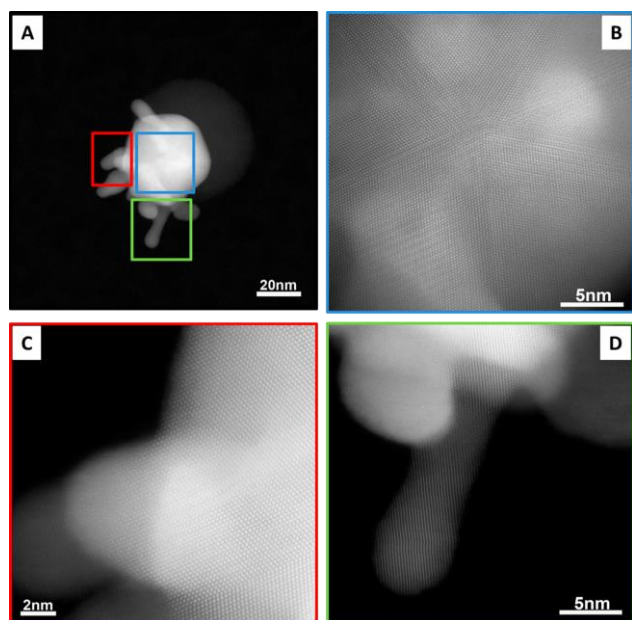
Fig. 3. **A**. HAADF-STEM image of a single Au-SiO$_2$ Janus nanostar with short spikes, revealing the presence of a gold core with branches (brighter feature) and also a SiO$_2$ shell at one side of the particle (less bright feature). **B-D**. HRSTEM images of the same particle showing that the Au core is multi-twinned whereas the branches seem to be single crystals.

Regarding the optical response of these anisotropic nanostructures, the Vis-NIR spectra of colloids obtained with different amounts of seeds (*Figure S2*) show that the main plasmon band redshifted further for lower amounts of seeds, which correlates well with the growth of longer branches, in agreement with previously reported theoretical modeling.[21,22,23,24] It should be noted that the amount of seeds is also a critical parameter to optimize branched growth without secondary nucleation. Paying more attention to the Vis-NIR spectra, one can see that they comprise two localized surface plasmon bands (LSPRs),[25] which is typical for star-like nanoparticles. One LSPR mode around 540 nm depends on core size, in this case determined by the original Janus seeds, whereas the second mode is focalized at the tips and its position can be tuned between 700-850 nm by simply changing the amount of seeds (and in turn branch dimensions). Other parameters such as the addition of hydrochloric acid or the amount of silver ions can also modify the morphology and affect LSPR position, but we have found that tuning the seeds concentration is a more reliable and reproducible strategy. When comparing these spectra with those of standard Au nanostars, it seems that the relative intensities between tip to core LSPR modes is lower in the Janus nanostars, which can be due to the smaller amount of branches per particle compared to fully spiked nanoparticles. This agrees with previous theoretical modelling indicating that the intensity of the tip mode is roughly proportional to the number of spikes.[18]

In summary, we have demonstrated the use of the protecting group concept for the synthesis of Janus nanoparticles comprising a spherical gold core half covered with a silica semishell and with gold tips branching out from the other half. Advances on the colloidal synthesis of Janus particles have allowed us to deposit the silica half shell on metallic spheres, and was then used as a hard mask to prevent the growth of gold spikes over the whole surface. This mask can be easily removed by dissolving silica in aqueous media, thus completing the similarity with protecting groups employed in Organic chemistry. These particles exhibit optical properties similar to those of gold nanostars in solution, but enhanced anisotropy can be expected for oriented assemblies by exploiting the Janus conformation. We have also shown that HAADF-STEM tomography and aberration corrected HAADF-STEM imaging are essential tools to understand the Janus morphology in detail. Future applications can be envisaged in the fields of surface enhanced spectroscopies or in the design of colloidal swimmers.

Notes and references

^{a} *BioNanoPlasmonics Laboratory, CIC biomaGUNE, Paseo de Miramón 182, 20009 Donostia – San Sebastián, Spain. Fax: 34 943005301; E-mail: llizmarzan@cicbiomagune.es.*

^{b} *EMAT-University of Antwerp, Groenenborgerlaan 171, B-2020, Antwerp, Belgium*

^{c} *Departamento de Química Física, Universidade de Vigo, 36310 Vigo, Spain*

^{d} *Ikerbasque, Basque Foundation for Science, Bilbao, Spain.*

1 G.M. Wuts, T.W. Greene, Protective Groups in Organic Synthesis, 4th ed., *John Wiley & Sons Inc.*, Hoboken, New Jersey, **2007**.

2 A. Perro, S. Reculusa, F. Pereira, M.-H. Delville, C. Mingotaud, E. Duguet, E. Bourgeat-Lamid, S. Ravaine, *Chem. Commun.* **2005**, 5542–5543.

3 X. Xu, N. L. Rosi, Y. Wang, F. Huo, C. A. Mirkin, *J. Am. Chem. Soc.* **2006**, 128, 9286-9287.

4 M. M. Maye, D. Nykypanchuk, M. Cuisinier, D. van der Lelie, O. Gang, *Nat. Mater.* **2009**, 8, 388-391.

5 F. Wang, S. Cheng, Z. Bao, J. Wang, *Angew. Chem. Int. Ed.* **2013**, 52, 1-6.

6 A. Guerrero-Martínez, M. Grzelczak, L.M. Liz-Marzán, *ACS Nano* **2012**, *6*, 3655-3662.

7 A. Guerrero-Martínez, S. Barbosa, I. Pastoriza-Santos, L.M. Liz-Marzán, *Curr. Op. Colloid Interface Sci.* **2011**, 16, 118-127.

8 D. Rodríguez-Fernández, L. M. Liz Marzán, *Part. Part. Syst. Charact.* **2013**, 30, 46–60.

9 N. G. Bastús, J. Comenge, V. Puntes, *Langmuir* **2011**, 27, 11098–11105.

10 G. Frens, *Nat. Phys. Sci.* **1973**, 241, 20.

11 T. Chen, G. Chen, S. Xing, T. Wu, H. Chen, *Chem. Mater.* **2010**, 22, 3826–3828.

12 L. M. Liz Marzán, M. Giersig, P. Mulvaney, *Langmuir* **1996**, 12, 4329-4335.

13 H. Yuan, C. G. Khoury, H. Hwang, C. M. Wilson, G. A. Grant, T. Vo-Dinh, *Nanotechnology* **2012**, 23, 075102.

14 S. Chen, Z. L. Wang, J. Ballato, S. H. Foulger, D. L. Carroll, *J. Am. Chem. Soc.* **2003**, 125, 16186-16187.

15 E. Hao, R. C. Bailey, G. C. Schatz, J. T. Hupp, S. Li, *Nano Lett.* **2004**, Vol. 4, 327-330.

16 T. K. Sau, C. J. Murphy, *J. Am. Chem. Soc.* **2004**, 126, 8648-8649.

17 J. Xie, J. Y. Lee, D. I. C. Wang, *Chem. Mater.* **2007**, 19, 2823-2830.

18 P. S. Kumar, I. Pastoriza-Santos, B. Rodríguez-González, F. J. García de Abajo, L. M. Liz-Marzán, *Nanotechnology* **2008**,19, 015606.

19 L. Rodríguez-Lorenzo, J. M. Romo-Herrera, J. Pérez-Juste, R. A. Álvarez-Puebla, L. M. Liz-Marzán, *J. Mater. Chem.* **2011**, 21, 11544.

20 Y. J. Wong, L. Zhu, W. S. Teo, Y. W. Tan, Y. Yang, C. Wang, H. Chen, *J. Am. Chem. Soc.* **2011**, 133, 11422–11425.

21 F. Hao, C. L. Nehl, J. H. Hafner, P. Nordlander, *Nano Lett.* **2007**, 7, 729-732.
22 W. Y. Ma, H. Yang, J. P. Hilton, Q. Lin, J. Y. Liu, L. X. Huang, J. Yao, *Opt. Express* **2010**, 18, 843-853.
23 S. Mazzucco, O. Stéphan, C. Colliex, I. Pastoriza-Santos, L. M. Liz-Marzán, J. García de Abajo, M. Kociak, *Eur. Phys. J. Appl. Phys.* **2011**, 54, 33512.
24 L. Shao, A. S. Susha, L. S. Cheung, T. K. Sau, A. L. Rogach, J. Wang, *Langmuir* **2012**, 28, 8979−8984.
25 L. M. Liz-Marzán, *Langmuir* **2006**, 22, 32-41.